# Numerical Analysis of Structures of Revolution using Universal Matrices Approach

Hamza Sulayman Abdullahi*

Department of Mechanical Engineering, Bayero University, Kano, 700241, Nigeria.

***ABSTRACT:*** Stress and displacement analysis of structures of revolution under axisymmetric loading is of considerable interest in engineering. Many practical problems can be idealized as an axisymmetric case, which simplifies the analysis and reduces the computational work. The axisymmetric triangular element is commonly used for modeling these cases. This paper proposes a method of generating stiffness matrix for the axisymmetric triangular element using universal matrices instead of numerical integration. The computation time of the proposed method was compared against the Gaussian numerical integration. The CPU time ratio for the 3-node element was 1:1.56, 1:1.79, and 1:1.89 for the proposed method against 1-point, 3-points, and 4-points Gaussian numerical integration respectively. The accuracy of the proposed method was 0.012% against the exact integration method. The 1-point, 3-points, and 4-points Gaussian numerical integration have an error of 0.059%, 0.001%, and 0.0006% respectively. Nodal displacements from this method were compared against the results of some commercially available finite element packages. The proposed method has a deviation of 0.44% from the theoretical values, while ABAQUS, ANSYS, and Optistruct has a deviation of 1.26%, 1.29%, and 1.44% respectively using the default number of integration points provided by the packages.

***KEYWORDS:*** Stiffness matrix; explicit formulation; closed-form; universal matrix; axisymmetric triangular elements.

[Received April 26, 2018; Revised August 10, 2018; Accepted September 19, 2018] Print ISSN: 0189-9546 | Online ISSN: 2437-2110

## I. INTRODUCTION

In Finite Element Analysis, some cases of 3D problems associated with the structures of revolution (SOR) can be reduced to a 2D problem by using axisymmetric elements, which simplifies the analysis and reduces computational work (Cui and Xu, 2013). These structures are generated by rotating a cross-section about an axis, as shown in

Figure **1**. The cross-section can be of any 2D shape; the resulting structure is said to be axisymmetric (O. C. Zienkiewicz *et al.*, 2014). These structures are paramount in engineering applications due to their ease of manufacture and optimality in strength-weight ratio, by hollowing the structure it can further be used as a container. Axles, bottles, cans, cups, nails, piles, pipes, tanks, vessels, and wheels are all examples of structures of revolution. In the transportation of fluids at different atmospheric conditions such structures are widely used (Gill, 1970).

For an axisymmetric structure to be defined as an axisymmetric problem, it is imperative that the boundary and loading conditions be rotationally symmetric, with these two conditions, the mechanical response of the structure is regarded as axisymmetric and the displacement, strains, and stress are not affected by the circumferential position (O. C. Zienkiewicz *et al.*, 2014).

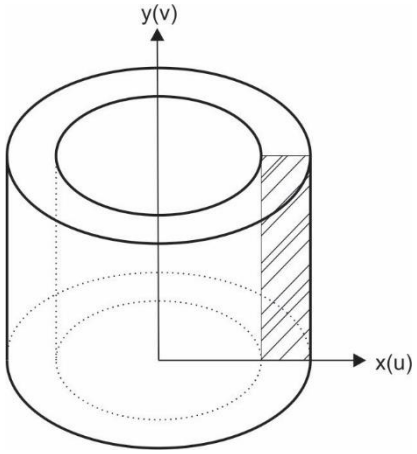


**Figure 1: Axisymmetric cylinder.**

The finite element technique predicts deformation and its intensity on a given structure, this is achieved by dividing the structure into a network of elements called mesh, the elements are non-complex shapes for which the finite element code can evaluate the stiffness matrix (Chandrupatla and Belegundu, 2001; Pachpor *et al.*, 2011). The nodes, which are the points at which the elements are connected are used to determine the unknown field variables such as displacement or temperature. Element stiffness matrices are further combined into a global stiffness matrix for the whole model

*Corresponding author: hsabdullahi.mec@buk.edu.ng

***doi:*** http://dx.doi.org/10.4314/njtd.v16i2.6

and then solved for the unknowns. Elements can either have a constant, linear or cubic strains within the element (Zienkiewicz *et al.*, 2005). The first archival-journal on the axisymmetric finite element using solid elements was applied to a rocket nozzle problem presented by Wilson (1965).

Shape functions are used to describe the elements behavior between element nodes (Huttton, 2004). The coefficients in the interpolation polynomial denote the shape function, which is written for each individual node of a finite element and its magnitude is 1 at that node and 0 for all other nodes in that element. The local coordinate system x and y can be converted into another coordinate system that allows for specifying a point within the element by a dimensionless number whose magnitude never exceeds unity called natural coordinate system (Huttton, 2004).

Numerical Integration has been widely applied in finite element analysis mainly due to its simplicity. It provides an approximate solution of the exact integration. Researchers over the past few decades have been studying and developing better approximation than the conventional numerical integration. An alternate method was presented by Subramanian (Subramanian and Bose, 1982) for plane triangular elements which result in a closed-form solution i.e. same as exact integration. Another method for computing stiffness matrix that results in closed-form solution and reduction in computational effort for quad elements was presented by Zhou and Vecchio (2006). McCaslin *et al.* (2012) considers isoparametric and subparametric higher order tetrahedral element and proposed yet another closed-form approach. Symbolic computation was used to reduce computation time by 50% for exact integration (Videla *et al.*, 2008). An alternate midpoint quadrature was suggested by Jeyakarthikeyan *et al.* (2017) to enhance the stiffness matrix of quad elements. For axisymmetric triangular element under axisymmetric loading, using a closed-form approach is possible only when the radius of the element is much larger than the element thickness (Subramanian and Bose, 1982; Jeyakarthikeyan *et al.*, 2015).

Familiarity with the stiffness matrix is essential to understanding the stiffness method. A stiffness matrix $[K]$ is a matrix such it relates the local forces $[F]$ on an element with the displacement $[u]$ on the nodes as $[F] = [K][u]$, the stiffness matrix indicates the defiance of the element to axial, bending, shear, or torsional deformation (Zienkiewicz *et al.*, 2005). In fluid flow and heat transfer analyses, the stiffness matrix represents the resistance of the element to change when subjected to motion or temperature gradient (O.C. Zienkiewicz *et al.*, 2014). Element stiffness matrices are always symmetric and positive for definitive structural problems, the diagonal coefficients are always positive and relatively large when compared to the off-diagonal values in the same row, it is banded and singular (Zienkiewicz *et al.*, 2005).

The objective of this paper is to generate stiffness matrix for the axisymmetric triangular element using universal matrices instead of numerical integration. First, the foundation of finite element formulation and the development of universal matrices is described. The accuracy and computation time of the proposed method was analyzed. Lastly, a linear-static finite element study of a cylinder subjected to internal pressure was carried out, the result from three commercially available packages was compared against the results of the proposed method.

## II. SYSTEM MODELLING

The axisymmetric triangular elements have 2 degrees of freedoms (u, v) per node which is represented by the nodal displacements. For the purpose of illustration in this paper, the three-node axisymmetric triangular element will be used, it is usually referred to as Constant Strain Triangle (CST) as the strain is constant along its sides. The radius of the element is approximated as

$$\bar{x} = \frac{1}{3}\sum_{1}^{3} x_i \tag{1}$$

where $x$ is the radial coordinate of the element nodes. The strain-displacement equation gives

$$\varepsilon = \begin{Bmatrix} \varepsilon_x \\ \varepsilon_y \\ \gamma_{xy} \\ \varepsilon_\theta \end{Bmatrix} = \begin{Bmatrix} \dfrac{\delta u}{\delta x} \\ \dfrac{\delta v}{\delta y} \\ \dfrac{\delta u}{\delta y} + \dfrac{\delta v}{\delta x} \\ \dfrac{u}{\bar{x}} \end{Bmatrix} \tag{2}$$

where $\varepsilon_x, \varepsilon_y, \varepsilon_\theta$ are the three normal strains and $\gamma_{xy}$ is the shear strain. The subscripts $x, y$ and $\theta$ denotes the radial, axial and tangential directions. The field variable (displacements) are denoted by $u$ and $v$. The shape functions for the CST are

$$\begin{aligned} N_1^* &= \xi, \\ N_2^* &= \eta, \\ N_3^* &= 1-\xi-\eta \end{aligned} \tag{3}$$

Where $\xi$ and $\eta$ are interpolating terms with values ranging from 0 to 1. For a 3-node CST element with the isoparametric formulation, the geometry ($x$ and $y$) and field variable ($u$ and $v$) are of the same order.

$$\begin{aligned} u &= N_1 u_1 + N_2 u_2 + N_3 u_3 \\ v &= N_1 v_1 + N_2 v_2 + N_3 v_3 \\ x &= N_1^* x_1 + N_2^* x_2 + N_3^* x_3 \\ y &= N_1^* y_1 + N_2^* y_2 + N_3^* y_3 \end{aligned} \tag{4}$$

The Jacobian matrix for the transformation is given by

$$[J] = \begin{bmatrix} \dfrac{\delta x}{\delta \xi} & \dfrac{\delta y}{\delta \xi} \\ \dfrac{\delta x}{\delta \eta} & \dfrac{\delta y}{\delta \eta} \end{bmatrix}$$

The strain-displacement equation becomes

$$\varepsilon = \frac{1}{2\Delta}[P][g] \qquad (5)$$

where $[P] = \begin{bmatrix} y_{23} & y_{13} & 0 & 0 & 0 \\ 0 & 0 & -x_{23} & x_{13} & 0 \\ -x_{23} & x_{13} & y_{23} & y_{13} & 0 \\ 0 & 0 & 0 & 0 & \frac{2\Delta}{\bar{x}} \end{bmatrix}$,

$x_{ij} = x_i - x_j$, $y_{ij} = y_i - y_j$, $[g]^T = \begin{bmatrix} \frac{\delta u}{\delta \xi} & \frac{\delta v}{\delta \eta} & \frac{\delta u}{\delta \xi} & \frac{\delta v}{\delta \eta} & u \end{bmatrix}$ and $\Delta$ is the area of the triangular element.

The internal energy of the element is given by $U = \frac{t}{2}\int_0^1\int_0^{1-\xi} \varepsilon^T [D]\varepsilon(2\Delta) d\xi d\eta$ where $t = 2\pi\bar{x}$ and $[D]$ is the elasticity matrix for axisymmetric problems.

Substituting the strain-displacement equation we have

$$U = \frac{\pi\bar{x}}{2\Delta}\int_0^1\int_0^{1-\xi} [g]^T [G][g]\, d\xi d\eta$$

Where $[G] = [P]^T [D][P]$ a 5 x 5 matrix of constants, we can also express $[g]^T$ as:

$$[g]^T = [u \quad v]^T [N']^T$$

$$[N']^T = \begin{bmatrix} \frac{\delta N}{\delta \xi} & 0 & \frac{\delta N}{\delta \eta} & 0 & N \\ 0 & \frac{\delta N}{\delta \xi} & 0 & \frac{\delta N}{\delta \eta} & 0 \end{bmatrix}$$

Which yields

$$U = \frac{\pi\bar{x}}{\Delta}\int_0^1\int_0^{1-\xi} [u \quad v]^T [N']^T [G][N'][u \quad v]\, d\xi d\eta$$

$$U = \frac{1}{2}[u \quad v]^T [K][u \quad v]$$

Where the stiffness matrix [K] is given by

$$[K] = \frac{\pi\bar{x}}{\Delta}\int_0^1\int_0^{1-\xi} [N']^T [G][N']\, d\xi d\eta \qquad (6)$$

The universal matrices are denoted by [A], [B], [C], [E], [H] and [J], they are the result of integration over the shape functions of the field variable (Abdullahi, 2015).

$$[A] = \int_0^1\int_0^{1-\xi} \frac{dN^T}{d\xi}\frac{dN}{d\xi} d\xi d\eta = \frac{1}{2}\begin{bmatrix} 1 & 0 & -1 \\ 0 & 0 & 0 \\ -1 & 0 & 1 \end{bmatrix}$$

$$[B] = \int_0^1\int_0^{1-\xi} \frac{dN^T}{d\xi}\frac{dN}{d\eta} d\xi d\eta = \frac{1}{2}\begin{bmatrix} 0 & 1 & -1 \\ 0 & 0 & 0 \\ 0 & -1 & 1 \end{bmatrix}$$

$$[C] = \int_0^1\int_0^{1-\xi} \frac{dN^T}{d\eta}\frac{dN}{d\eta} d\xi d\eta = \frac{1}{2}\begin{bmatrix} 0 & 0 & 0 \\ 0 & 1 & -1 \\ 0 & -1 & 1 \end{bmatrix}$$

$$[E] = \int_0^1\int_0^{1-\xi} N^T N\, d\xi d\eta = \frac{1}{24}\begin{bmatrix} 2 & 1 & 1 \\ 1 & 2 & 1 \\ 1 & 1 & 2 \end{bmatrix}$$

$$[H] = \int_0^1\int_0^{1-\xi} N^T \frac{dN}{d\xi} d\xi d\eta = \frac{1}{6}\begin{bmatrix} 1 & 0 & -1 \\ 1 & 0 & -1 \\ 1 & 0 & -1 \end{bmatrix}$$

$$[J] = \int_0^1\int_0^{1-\xi} N^T \frac{dN}{d\eta} d\xi d\eta = \frac{1}{6}\begin{bmatrix} 0 & 1 & -1 \\ 0 & 1 & -1 \\ 0 & 1 & -1 \end{bmatrix}$$

Substituting the universal matrices into equation (6), the element stiffness matrix of the 3-noded constant strain triangle (CST) can be written as:

$$[K] = \frac{\pi\bar{x}}{\Delta}\begin{bmatrix} X & Y \\ Y^T & Z \end{bmatrix} \qquad (7)$$

where

$$X = G_{11}[A] + G_{12}[B + B^T] + G_{22}[C] + G_{25}[J + J^T] + G_{15}[H + H^T] + G_{55}[E]$$

$$Y = G_{13}[A] + G_{23}[B^T] + G_{53}[H] + G_{14}[B] + G_{54}[J] + G_{24}[C]$$

$$Z = G_{33}[A] + G_{43}[B + B^T] + G_{44}[C]$$

$G_{ij}$ are the terms of the $[G]$ matrix.

An algorithm was developed to explicitly compute the stiffness matrix terms and save it in memory for retrieval, these explicit equations will be used instead of evaluating the integrals or matrix multiplication when solving the problem, therefore the stiffness matrix becomes a simple algebraic computation and reduces the computation time.

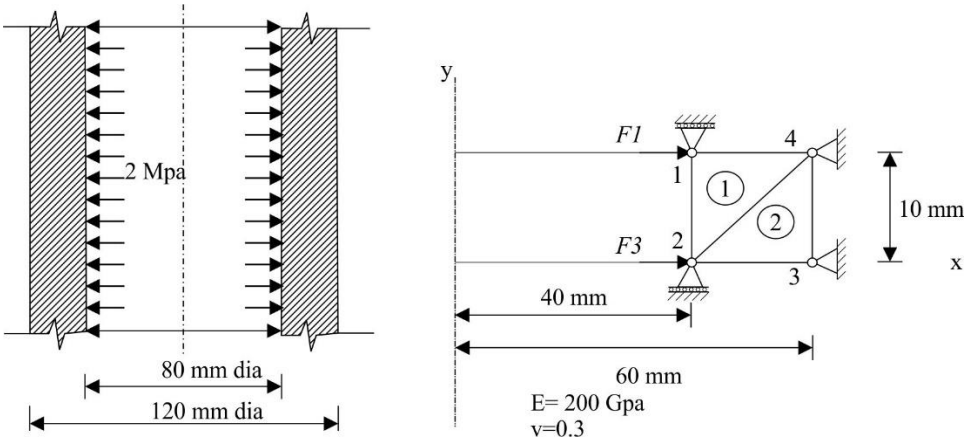


**Figure 2: Axisymmetric problem formulation (Chandrupatla and Belegundu, 2001).**

An axisymmetric problem (Figure 2) which consists of a cylinder subjected to internal pressure was used to assess the capability of the method presented in this paper. The cylinder has an internal diameter of 80mm and an external diameter of 120mm subjected to internal pressure of 2MPa, the Young modulus of the cylinder wall material is 200Gpa with a Poisson ratio of 0.3.

The axisymmetric problem depicted in Figure 2 was modeled using three finite element packages; ABAQUS, ANSYS, and Optistruct. Modeling procedure for each package is explained in the following subsections. The material of the cylinder wall has a Young Modulus of 200 GPA and Poisson Ratio of 0.3.

A linear-static analysis was employed using Abaqus/Standard (ABAQUS, 2015). The part was set to be a deformable axisymmetric shell, an isotropic elastic property was defined. A general static step was created. A three-node linear stress/displacement element without twist (CAX3) was used to mesh the model, the model consists of 2 elements and 4 nodes. Fixed boundary conditions were employed on the outer radius nodes while the inner nodes are only allowed to move in a radial direction. The inner radius edge was subjected to a uniform pressure of 2Mpa.

A static analysis using Plane182 element was employed, the element is a four-node rectangular element that was further degenerated to a triangular element by merging the last two nodes (ANSYS, 2013). The axisymmetric option was selected along with full integration and pure displacement. An isotropic elastic property was defined. Uniform pressure of 2MPa was resolved into forces and applied on the inner radius nodes.

Axisymmetric triangular element CTAXI was used to define the problem, all the nodes were placed on the x-z plane with x as the radius. The pressure was applied using PLOADX1, which is a bulk unsupported card for static pressure load on axisymmetric elements. Material and property were defined as MAT1 and PAXI cards respectively. A linear static load step with two set of constraints for the inner and outer radius was defined.

## IV. RESULTS AND DISCUSSION

### *A. Accuracy and Computation Time*

In non-axisymmetric triangular elements, the Universal Matrix Method (UMM) gives the exact solution (Subramanian and Bose, 1982). Due to the approximation of the radius of the element shown in equation (1) the proposed method gives another approximation. Therefore, the need for determining the deviation of UMM and numerical integration from the exact integration becomes paramount.

To assess the computational efficiency of the proposed method, we consider the cylinder in Figure 2 and compute the stiffness matrices using the universal matrices and Gaussian numerical integration for the 3-node (CST) and the 6-node (LST) axisymmetric triangular elements. The CPU time is taken for 10,000 elements. The numerical integration was coded as explicit equations this is aimed at providing a common ground for the execution time comparison.

The test was carried out on a desktop computer with Intel® Core™ CPU i5-6400 (2.70 GHz) and 16GB of RAM running on a 64-Bit Windows operating system for all the steps to ensure a fair comparison. For each of the elements a problem is solved using the methods and then the stiffness matrix generated is compared and the error is estimated using the expression presented by Videla *et al.* (2008) as follows

$$e = \frac{\sqrt{\sum_{i,j=1}^{n}\left(K_{ij}^{T} - K_{ij}\right)}}{\sum |K_{ij}^{T}|} \times 100 \qquad (8)$$

where $K_{ij}^{T}$ the stiffness matrix is terms using exact integration and $K_{ij}$ is the stiffness matrix term using UMM or Gaussian numerical integration. The CPU time ratio for element 1 with radius $\bar{x}$ = 46.67mm is shown in Table 1.

**Table 1: Computation time ratio for 10,000 elements.**

| Elements | Method | CPU time ratio |
|---|---|---|
| CST | Current Work | 1.00 |
| | NI 1 point | 1.56 |
| | NI 3 points | 1.79 |
| | NI 4 points | 1.89 |
| LST | Current Work | 1.00 |
| | NI 1 point | 5.64 |
| | NI 3 points | 12.84 |
| | NI 4 points | 16.69 |
| | NI 7 points | 28.12 |

The CPU time ratio for the 3-node CST element was 1.00 for UMM while Gaussian numerical integration has 1.56, 1.79 and 1.89 for 1-point, 3-points, and 4-points integration respectively. The computation time increases with an increase in the number of points due to re-computation loop for each point and then taking the weighted sum. While UMM uses only one computation loop. Similarly, for the 6-node LST element, the CPU time ratio was 1.00 for the universal matrix method and 5.64, 12.84, 16.69 and 28.12 for 1-point, 3-points, 4-points, and 7-points Gaussian numerical integration.

Figure 2 shows the percentage error for UMM and Gaussian numerical integration with 1, 3 and 4 points against the exact integration. CST elements with radius $\bar{x}$ = 46.67mm and 53.33mm were used for the cylinder problem shown in Figure 2. The result indicated that UMM has a better approximation (0.012% error) than the 1-point numerical integration (0.059%) which is the most commonly used by commercial packages. However, by increasing the number of integration points to 3 and 4 the error drastically decreases to 0.001% and 0.0006% respectively. This clearly shows that when using a 3-node constant strain triangle, a minimum of 3 points is required in the commercial finite element packages.

Figure 4 shows the percentage error for UMM and Gaussian numerical integration with 1, 3, 4 and 7 points against exact integration. Six-node linear strain triangle

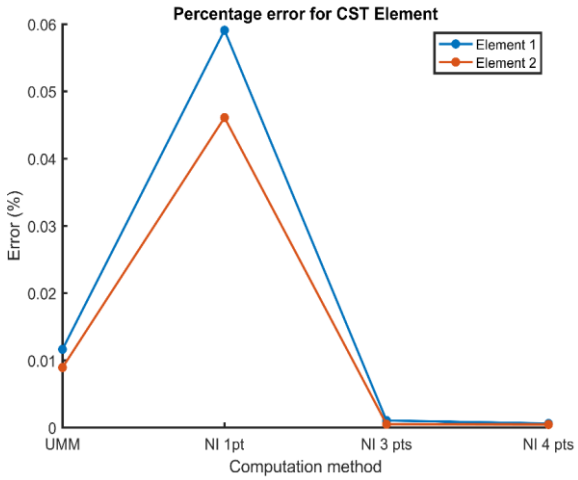


**Figure 2: Percentage Error for CST using UMM and Numerical Integration.**

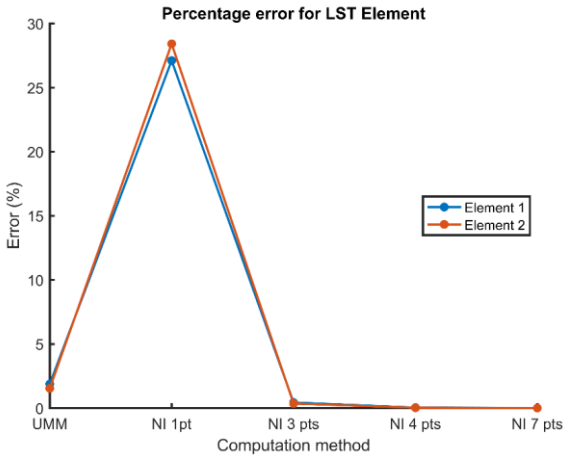


**Figure 4: Percentage Error for LST using UMM and Numerical Integration.**

(LST) elements with radius $\bar{x}$ = 46.67mm and 53.33mm were used for the cylinder problem shown in Figure 2. Three mid-nodes are added to the CST to create the LST. The result indicated that UMM has a better approximation (1.873% error) than the 1-point numerical integration (27.1%). However, by increasing the number of integration points to 3, 4 and 7 the error drastically decreases to 0.43%, 0.032%, and 0.00015% respectively. This clearly shows that when using a 6-node linear strain triangle, a minimum of 3 points is required in the commercial finite element packages.

*B. Nodal Displacement*

The axisymmetric problem illustrated in Figure 2 was solved using the explicit equations generated. To further understand the computational accuracy of the proposed method, the nodal displacements from the current work, ABAQUS, ANSYS, and Optistruct was compared against the theoretical values obtained using exact integration. The result for node 1 of element 1 is shown in Figure 5.

The universal matrix method has a deviation of 0.44% from the theoretical values, while ABAQUS, ANSYS, and Optistruct has a deviation of 1.26%, 1.29%, and 1.44% respectively using the default number of integration points provided by the packages. A similar trend was observed on node 2 as shown in Figure . The deviation of the current work from the theoretical values on the second node displacement is 0.54%, while ABAQUS, ANSYS, and Optistruct have a deviation of 1.62%, 1.64%, and 1.84% respectively using the default number of integration points provided by the packages. These deviations shown by the commercial packages considered in this study is highly associated with fewer integration points for the numerical integration of the shape functions.

ABAQUS uses 1-point integration for the 3-node linear axisymmetric triangular element (CAX3). The 6-node quadratic axisymmetric triangular element (CAX6) and the 4-node bilinear axisymmetric quadrilateral element (CAX4) are recommended by ABAQUS because of the number of integration points (ABAQUS, 2015). The CAX6 uses 3 integration points while the CAX4 has the option for full (4-point) and reduced (1-point) integration. ANSYS and Optistruct both use 1-point integration for the Plane182 and CTAXI elements. ANSYS recommends using the 4-node version of Plane182 without degeneration (ANSYS, 2013).

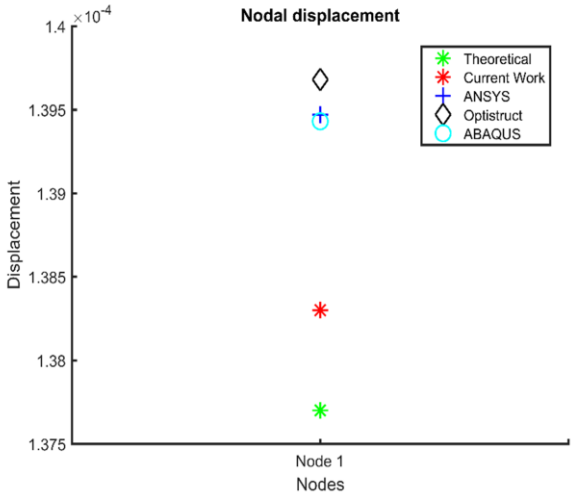


**Figure 5: Displacement of node 1.**

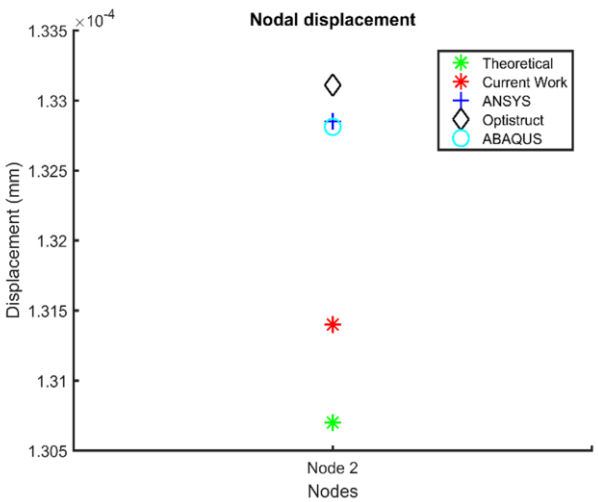


**Figure 6: Displacement of Node 2.**

## V. CONCLUSION

A method of generating stiffness matrix for triangular axisymmetric elements was presented, the method utilizes universal matrices generated by integrating the shape functions once and saved for retrieval in memory. Furthermore, a set of explicit equations were generated for each term of the stiffness matrix to improve the computational efficiency. Unlike other closed-form approaches to finite elements, the stiffness matrix computation method presented in the current work results in yet another approximation, due to the element radius estimation.

However, the method shows a better approximation to the theoretical baseline, with better acceptable percentage error and lower computation time. The proposed method has a deviation of 0.44% and 0.54%, while the commercial finite element packages considered in this work have deviations up to 1.44% with the default number of integration points. Increasing the number of the integration points decreases the error significantly and increases the computation time. Therefore, careful consideration should be given when choosing the element and the number of points to find a balance between accuracy and computation time.

## REFERENCES

**ABAQUS. (2015)**. ABAQUS User's Guide. Dassault Systèmes, Providence, RI, USA.

**Abdullahi, H. S. (2015)**. Time efficiency analysis and error estimation in generating element stiffness matrices of axisymmetric plane triangular elements using universal matrix method. Department of Mechanical Engineering, SRM University, Chennai, India.

**ANSYS. (2013).** ANSYS Mechanical APDL Theory Reference, ANSYS Inc.pp. 1–909. Available at: www.ansys.com.

**Chandrupatla, T. R. and Belegundu, A. (2001).** Introduction to Finite Elements in Engineering. Prentice Hall, Upper Saddle River, New Jersey.

**Cui, D. and Xu, Y. M. (2013).** Finite element analysis in engineering. Beihang University Press, Beijing, China.

**Gill, S. (1970).** The stress analysis of pressure vessels and pressure vessel components. Pergamon Press.

**Huttton, D. V. (2004)**. Fundamentals of Finite Element Analysis. McGraw-Hill.

**Jeyakarthikeyan, P. V.; G. Subramanian and R. Yogeshwaran. (2017).** An alternate stable midpoint quadrature to improve the element stiffness matrix of quadrilaterals for application of functionally graded materials (FGM), Computers & Structures, 178:71–87. doi: 10.1016/j.compstruc.2016.10.008.

**Jeyakarthikeyan, P. V.; R. Yogeshwaran and H. S. Abdullahi. (2015)**. Time efficiency and error estimation in generating element stiffness matrices of plane triangular elements using Universal Matrix Method and Gauss-Quadrature, Ain Shams Engineering Journal, 9 (4): 965-972.

**McCaslin, S. E.; P. S. Shiakolas, B. H. Dennis, and K. L. Lawrence. (2012).** Closed-form stiffness matrices for higher order tetrahedral finite elements, Advances in Engineering Software, 44(1):75–79.

**Pachpor, P. D.; N. D. Mittal, L. N. Gupla, and N. V. Deshpande. (2011).** Finite element analysis and comparison of castellated & cellular beam, Advanced Materials Research, 264–265(1):649–699. doi: 10.4028/www.scientific.net/AMR.264-265.694.

**Subramanian, G. and Bose, C. J. (1982)**. Convenient generation of stiffness matrices for the family of plane triangular elements, Computers and Structures, 15(1): 85–89. doi: 10.1016/0045-7949(82)90036-0.

**Videla, L.; T. Baloa, D. V. Griffiths and M. Cerrolaza. (2008).** Exact integration of the stiffness matrix of an 8-node plane elastic finite element by symbolic computation, Numerical Methods for Partial Differential Equations, 24(1):249–261.

**Wilson, E. L. (1965)**. Structural analysis of axisymmetric solids. American Institute of Aeronautics and Astronautics Journal, 3(12): 2269–2274. doi: 10.2514/3.3356.

**Zhou, C. E. and Vecchio, F. J. (2006).** Closed-Form Stiffness Matrix for the Four-Node Quadrilateral Element with a Fully Populated Material Stiffness, Journal of Engineering Mechanics, 132(12): 1392–1395. doi: 10.1061/(ASCE)0733-9399(2006)132:12(1392).

**Zienkiewicz, O. C.; R. L. Taylor, and D. Fox. (2013).** The Finite Element Method for Solid and Structural Mechanics, 7th Ed., Butterworth-Heinemann, USA.

**Zienkiewicz, O. C.; R. L. Taylor, and P. Nithiarasu. (2014).** The Finite Element Method for Fluid Dynamics, 7th Ed., Butterworth-Heinemann, USA.

**Zienkiewicz, O. C., Taylor, R. L. and Taylor, R. L. (2005).** The Finite Element Method for Solid and Structural Mechanics, Elsevier, Oxford, UK.